

From Cavitation to Astrophysics: Explicit Solution of the Spherical Collapse Equation

Danail Obreschkow^{1,2}

¹ *International Centre for Radio Astronomy Research, M468, Uni. of Western Australia, 35 Stirling Hwy, Perth, WA 6009, Australia*

² *International Space Centre, M468, University of Western Australia, 35 Stirling Hwy, Perth, WA 6009, Australia*

15 January 2024

ABSTRACT

Differential equations of the form $\ddot{R} = -kR^\gamma$, with a positive constant k and real parameter γ , are fundamental in describing phenomena such as the spherical gravitational collapse ($\gamma = -2$), the implosion of cavitation bubbles ($\gamma = -4$) and the orbital decay in binary black holes ($\gamma = -7$). While explicit elemental solutions exist for select integer values of γ , more comprehensive solutions encompassing larger subsets of γ have been independently developed in hydrostatics (see Lane-Emden equation) and hydrodynamics (see Rayleigh-Plesset equation). This paper introduces a general explicit solution for all real γ , employing the quantile function of the beta distribution, readily available in most modern programming languages. This solution bridges between distinct fields and reveals insights, such as a critical branch point at $\gamma = -1$, thereby enhancing our understanding of these pervasive differential equations.

Key words: gravitation, hydrodynamics, black hole physics, cosmology: theory

1 INTRODUCTION

It may be surprising that the 21st century still holds critically important differential equations, which admit rather straightforward, but barely known explicit solutions. In this paper, I discuss such a family of equations that govern all physical systems described by a one-dimensional time-dependent coordinate $R(T)$, subject to a restoring force that varies as a power law of that coordinate. Formally, this is expressed by the non-linear ordinary differential equation (ODE)

$$\ddot{R} = -kR^\gamma \quad (1)$$

with fixed $k \in \mathbb{R}_+$ and $\gamma \in \mathbb{R}$. Dots denote derivatives with respect to time T . Hereafter, I call Equation (1) the ‘spherical collapse’ equation as it is often used in this context.

I will restrict the discussion to the case, where R exhibits a finite maximum R_0 at some finite time—in many applications this is equivalent to stating that the system is ‘bound’ with negative total energy. Equation (1) being an autonomous ODE, we can always choose the origin of time to coincide with $R = R_0$, in which case the initial conditions read

$$R(0) = R_0 \quad \text{and} \quad \dot{R}(0) = 0. \quad (2)$$

Equations (1) and (2) are manifestly time-symmetric, i.e., $R(T) = R(-T)$ where a solution exists. Often most relevant is the time interval $T \in [0, T_c]$, from the maximum radius to the (first) collapse point, $R(T_c) = 0$. I will focus on this interval for most of this paper.

Table 1 lists various examples of physical systems governed by Equation (1). One of the most famous cases in astrophysics is the gravitational collapse of a uniform collisionless sphere ($\gamma = -2$), the so-called top-hat spherical collapse model (Gunn & Gott 1972). A simple parametric solution,

$\{T(\theta), R(\theta)\}$ (Lin et al. 1965), has become the default textbook solution. Its transcendental nature implies that algebraic solutions of Equation (1) do not generally exist, yet the search for explicit non-algebraic solutions and fast approximations continues, e.g., Slepian & Philcox (2023), who applied Fourier expansions to complex contour integration.

Barely known to astrophysicists, an analogous collapse equation (but with $\gamma = -4$) has long been studied in hydrodynamics. This equation, dating back to Stokes (1847) and Rayleigh (1917), describes the collapse of an empty spherical cavity in an ideal incompressible liquid. Approximate solutions $R(T)$ derived by Obreschkow et al. (2012) have led Amore & Fernández (2013) to develop an infinite series that rapidly converges towards the exact solution. Shortly after, Kudryashov & Sinelshchikov (2014, 2015) presented the first closed-form solution $T(R)$ for cavities in $N \geq 3$ dimensions, in terms of hypergeometric functions. These can, in principle, be inverted to explicit solutions $R(T)$.

Equation (1) is also encountered in static systems. For example, it is analogous to the one-dimensional Lane-Emden equation (Lane 1870; Emden 1907), describing the density profile of a self-gravitating polytropic gas in a thin tube in hydrostatic equilibrium. A solution for $\gamma > -1$ was presented by Harrison & Lake (1972) in the context of galactic discs.

Building on the special solutions found independently in different fields, this paper presents a general explicit solution of Equation (1) for any real γ . This solution constitutes a mathematical unification of a wide range of unrelated topics in physics and astrophysics. Section 2 overviews basic reformulations, useful for the derivation of the general solution in Section 3 and its discussion in Section 4. Section 5 concludes with a brief synthesis and outlook.

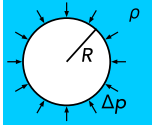
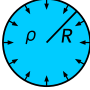
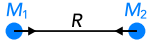
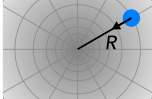
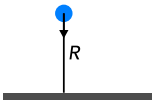
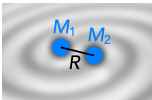
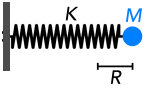
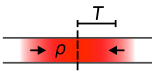
Physical system	Schematic	Meaning of R	Time scale T_0	γ	τ
Cavitation bubble Spherical cavity of constant (possibly zero) internal pressure, imploding under the pressure of an incompressible inviscid liquid without surface tension		Bubble radius	$R_0 \sqrt{\rho/\Delta p}$, where ρ is the density of the liquid and $\Delta p = p_\infty - p_v$, with far-field liquid pressure p_∞ and constant bubble pressure p_v	-4	≈ 0.91468
Generalisation to a spherical bubble in $N \geq 3$ dimensions (e.g., Klotz 2013)			$(N-2)^{-1/2} R_0 \sqrt{\rho/\Delta p}$	$-N-1$	(Eq. 21)
Gravitational collapse Collapse of a uniform sphere, also known as spherical top-hat, subjected only to gravitational forces		Radius of sphere	$\sqrt{3/(4\pi G \rho_0)}$, where ρ_0 is the initial density at the onset of the collapse and G is the gravitational constant	-2	$\pi/\sqrt{8} \approx 1.11072$
Two-body collision Two point masses in gravitational free-fall towards each other, on a straight line without angular momentum		Distance between the centres of the two masses	$R_0^{3/2}/\sqrt{G(M_1+M_2)}$, where M_i denote the two masses and G is the gravitational constant	-2	$\pi/\sqrt{8} \approx 1.11072$
Free-fall in spherical potential Radial free-fall in a spherically symmetric gravitational power law potential, $\phi \sim R^\alpha$, with index $\alpha \neq 0$		Distance from centre of potential	$\sqrt{(L/R_0)^\alpha/\alpha} \cdot R_0/V$, where L and V are the length and velocity scales of the potential $\phi(R) = \text{sgn}(\alpha) \cdot V^2 \cdot (R/L)^\alpha$	$\alpha-1$	(Eq. 21)
Same for a logarithmic potential, e.g., the potential of a singular isothermal sphere			R_0/V , where V is the velocity scale in $\phi(R) = V^2 \ln(R/L)$	-1	$\sqrt{\pi/2} \approx 1.25331$
Free-fall with constant acceleration Straight fall in a constant acceleration field, such as a vertical drag-free drop of an object on Earth		Height from the ground	$\sqrt{R_0/g}$, where g is the norm of the constant acceleration, e.g., $g = 9.81 \text{ m s}^{-2}$ on Earth	0	$\sqrt{2} \approx 1.41421$
Relativistic orbital decay Orbital decay by gravitational radiation of two masses at non-relativistic velocities, initially forced on circular orbits		Distance between the centres of the two masses	$\frac{5c^5 R_0^4}{64\sqrt{3}G^3 M_1 M_2 (M_1+M_2)}$, with M_i the two masses, G the gravitational constant and c the speed of light	-7	≈ 0.74683
Harmonic oscillator Motion of a mass attached to an ideal spring, initially at rest in an extended or compressed state		Distance from the equilibrium position	$\sqrt{M/K}$, where M is the mass and K the spring constant	+1	$\pi/2 \approx 1.57080$
Polytrope Density profile of a self-gravitating polytropic gas in one dimension in hydrostatic equilibrium		$\rho^{1/n}$, where ρ is the gas density and n the index of $p = K\rho^{1+1/n}$	$\sqrt{(1+n)KR_0^{1-n}/(4\pi G)}$ is a length scale set by the parameters of the polytropic equation of state $p = K\rho^{1+1/n}$	n	(Eq. 21)

Table 1. Examples of systems governed by Equations (1) and (2). Moving objects described by $R(T)$ are shown in blue, whereas static objects described by this equation are shown in red. T_0 is the characteristic physical scale (normally a characteristic time), such that Equation (1) reduces to the dimensionless Equation (5) upon normalisation via Equation (3). The collapse time is T_c , satisfying $R(T_c) = 0$, is given by $T_0\tau$. Where T_0 depends on R_0 , the latter is the maximum, initial value of R . In the case of the polytrope (bottom row), R and T have different meanings: $R := \rho^{1/n}$ is a measure of the gas density and T is the distance from the centre of mass. For most examples, analogous cases with other forces, such as electric forces instead of gravitational ones, can be found.

2 SETTING THE STAGE

Before delving into the solutions of Equation (1), it is worth stating a few straightforward, but pivotal remarks on equivalent reformulations. These will help the derivation (Section 3) and discussion (Section 4) of the solutions.

2.1 Dimensionless form

The first remark is that it is often more convenient to work in dimensionless position and time coordinates, defined as

$$r := \frac{R}{R_0} \quad \text{and} \quad t := \frac{T}{T_0}, \quad (3)$$

where $R_0 = R(0)$ is the maximum, initial value of R (c.f., Equation 2) and

$$T_0 := \sqrt{k^{-1}R_0^{1-\gamma}} \quad (4)$$

is the natural time constant. With this normalisation, Equation (1) becomes

$$\ddot{r} = -r^\gamma, \quad (5)$$

and the initial conditions (Equation 2) become

$$r(0) = 1 \quad \text{and} \quad \dot{r}(0) = 0. \quad (6)$$

It is understood that dots above $r(t)$ now denote derivatives with respect to t , rather than T . To help the following derivations, we introduce the variable $\tau := T_c/T_0$ as a shorthand for the dimensionless collapse time.

The constant k has conveniently disappeared in the dimensionless form of Equation (5), reducing the family of ODEs to a single control parameter γ . The natural disappearance of k brings to light the inherently scale-free nature of Equation (1) implied by its power law structure. This scale-invariance is the deeper reason for Equation (1) to be applicable from microscopic to astrophysical scales.

As a simple example, let us consider the gravitational collapse of a uniform pressure-free sphere, initially at rest with radius $R(0) = R_0$. The Newtonian equation of motion,

$$\frac{d^2 R}{dT^2} = -\frac{GM}{R^2}, \quad (7)$$

is identical to Equation (1) with constants $\gamma = -2$ and $k = GM$. Hence, the natural time constant is $T_0 = \sqrt{R_0^3/(GM)}$. Upon expressing R and T in their natural units R_0 and T_0 , Equation (7) becomes indeed $\ddot{r} = -r^{-2}$.

For convenience, the remainder of this paper will focus on dimensionless solutions $r(t)$. Corresponding dimensional solutions $R(T)$ are easily obtained using (Equation 3), given the scales R_0 and T_0 . Explicit expressions for these scales in various physical systems are provided in Table 1.

2.2 Equivalent formulations

The second remark is that Equation (5), and thus Equation (1), can be rewritten in other differential forms.

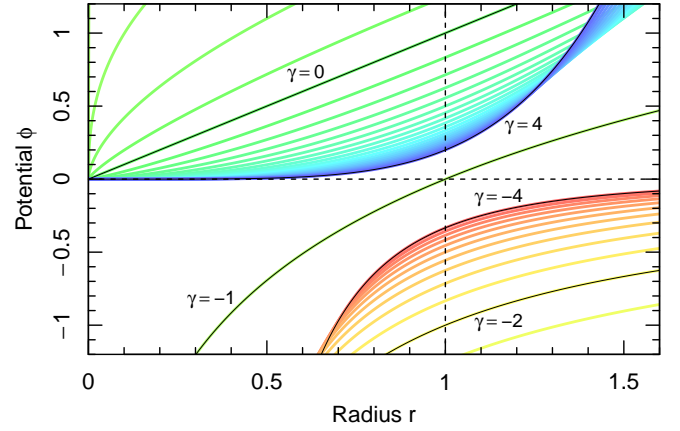


Figure 1. Potential $\phi(r)$, given in Equation (12), for different values of γ , equally spaced by $\Delta\gamma = 0.2$. There are qualitatively distinct families at $\gamma < -1$ (red–yellow) and $\gamma > -1$ (blue–green), as discussed in Section 4.1. They are separated by an isolated critical curve for $\gamma = -1$. Thin black lines highlight the coloured curves with a printed γ -value.

2.2.1 Integral of motion

Most importantly, Equation (5) always exhibits an *integral of motion*,

$$0 = \begin{cases} \frac{1+\gamma}{2} \dot{r}^2 + r^{1+\gamma} - 1 & \text{if } \gamma \neq -1 \\ \dot{r}^2 + 2 \ln r & \text{if } \gamma = -1 \end{cases} \quad (8a)$$

$$(8b)$$

If differentiated with respect to time and solved for \ddot{r} , Equation (8) becomes Equation (5). Strictly, this is true if and only if $\dot{r} \neq 0$, as the transition involves a division by \dot{r} . Since Equations (8) are first-order differential equations, only one boundary condition is required, such as $r(0) = 1$.

2.2.2 Hybrid differential equation

If $\gamma \neq -1$, a hybrid differential equation, mixing first and second derivatives, can be obtained by rewriting $r^{1+\gamma}$ in Equation (8a) as $rr^\gamma = -r\ddot{r}$ (Equation 5), hence

$$1 - \frac{1+\gamma}{2} \dot{r}^2 + r\ddot{r} = 0. \quad (9)$$

This is, for example, the standard form of the equation describing the collapse of a spherical cavitation bubble without viscosity and surface tension (Rayleigh 1917). This equation is normally written in dimensional form,

$$\frac{3}{2} \left(\frac{dR}{dT} \right)^2 + R \frac{d^2 R}{dT^2} + \frac{\Delta p}{\rho} = 0, \quad (10)$$

where Δp is the driving pressure and ρ the constant liquid density (see first row in Table 1). If normalising R by $R_0 = R(0)$ and T by $T_0 = R_0 \sqrt{\rho/\Delta p}$, Equation (10) becomes Equation (9) with $\gamma = -4$. It follows that Equation (10) is equivalent to Equation (1) with $\gamma = -4$ and $k = R_0^3 \Delta p / \rho$.

2.2.3 Lagrangian

Finally, with an eye on applications in physics, it is worth noting that Equation (5) derives from a time-independent Lagrangian

$$\mathcal{L}(r, \dot{r}) = \frac{\dot{r}^2}{2} - \phi(r) \quad (11)$$

with the potential, defined up to an additive constant,

$$\phi(r) = \begin{cases} r^{1+\gamma}/(1+\gamma) & \text{if } \gamma \neq -1 \\ \ln r & \text{if } \gamma = -1 \end{cases} \quad (12)$$

Applying the Euler-Lagrange equation, $\frac{d}{dt}(\partial\mathcal{L}/\partial\dot{r}) = \partial\mathcal{L}/\partial r$, generates Equation (5), for all γ .

Selected potentials $\phi(r)$ are shown in Figure 1. The existence of two regimes, separated by the critical value $\gamma = -1$, is the fundamental reason for the qualitatively different behaviour of $r(t)$ in these regimes. These regimes will be discussed in more detail in Section 4.1.

3 GENERAL SOLUTION

In this section, I derive compact general solutions of Equation (1) with initial conditions of Equation (2), following an approach similar to [Kudryashov & Sinelshchikov \(2014\)](#), but for general real parameters γ . For convenience, all derivations and solutions are presented for the dimensionless form in Equation (5) with initial conditions stated in Equation (6). Any solution $r(t)$ can be transformed to the corresponding dimensional solution $R(T)$ via the straightforward linear transformations of Equation (3).

3.1 Implicit solution $t(r)$

3.1.1 Cases $\gamma \neq -1$

Equation (8a) can be rewritten to separate time from position coordinates,

$$dt^2 = \frac{1+\gamma}{2(1-r^{1+\gamma})} dr^2. \quad (13)$$

During the collapse ($0 < r < 1$), the RHS is positive for any $\gamma \neq -1$. Since the collapse is characterised by a shrinking radius ($dr < 0$) with growing time ($dt > 0$), we are interested in the negative branch,

$$dt = - \left[\frac{1+\gamma}{2(1-r^{1+\gamma})} \right]^{1/2} dr. \quad (14)$$

Let us integrate this equation backward in time from the dimensionless collapse time τ to an earlier time $t > 0$,

$$\int_{\tau}^t dt = - \left[\frac{|1+\gamma|}{2} \right]^{1/2} \int_0^{r(t)} \frac{dr}{|1-r^{1+\gamma}|^{1/2}}. \quad (15)$$

The lower bound of the second integral is zero by definition of the collapse time. To simplify the notation of the following equations let us introduce the positive constant

$$\eta = \frac{1}{|1+\gamma|}, \quad (16)$$

and let $s := r^{|1+\gamma|} \in [0, 1]$. With these substitutions, $r = s^\eta$ and $dr = \eta s^{\eta-1} ds$, and hence

$$\int_{\tau}^t dt = - \sqrt{\frac{\eta}{2}} \int_0^{s(t)} \frac{s^{\eta-1} ds}{|1-s^{\pm 1}|^{1/2}}, \quad (17)$$

where the sign of the exponent in the denominator is equal to the sign of $1+\gamma$. If this sign is negative, we multiply the numerator and denominator of the fraction by $s^{1/2}$. Then,

$$\int_{\tau}^t dt = - \sqrt{\frac{\eta}{2}} \int_0^{s(t)} \frac{s^{\alpha-1} ds}{(1-s)^{1/2}}, \quad (18)$$

γ	τ (exact)	τ (num)	$\dot{r}(\tau)$ (exact)	$\dot{r}(\tau)$ (num)
$-\infty$	0	0	$-\infty$	$-\infty$
-100	—	0.22019512	$-\infty$	$-\infty$
-10	—	0.64597784	$-\infty$	$-\infty$
-4	—	0.91468136	$-\infty$	$-\infty$
-3	1	1	$-\infty$	$-\infty$
-2	$\pi/\sqrt{8}$	1.11072073	$-\infty$	$-\infty$
-5/3	$2/\sqrt{3}$	1.15470054	$-\infty$	$-\infty$
-3/2	$3\pi/8$	1.17809725	$-\infty$	$-\infty$
-4/3	$\pi\sqrt{75/512}$	1.20239047	$-\infty$	$-\infty$
-1	$\sqrt{\pi/2}$	1.25331414	$-\infty$	$-\infty$
-2/3	$\sqrt{128/75}$	1.30639453	$-\sqrt{6}$	-2.44948974
-1/2	4/3	1.33333333	-2	-2
-1/3	$\pi\sqrt{3}/4$	1.36034952	$-\sqrt{3}$	-1.73205081
0	$\sqrt{2}$	1.41421356	$-\sqrt{2}$	-1.41421356
1	$\pi/2$	1.57079633	-1	-1
2	—	1.71731534	$-\sqrt{2/3}$	-0.81649658
3	—	1.85407468	$-1/\sqrt{2}$	-0.70710678
4	—	1.98232217	$-\sqrt{2/5}$	-0.63245553
10	—	2.62843161	$-\sqrt{2/11}$	-0.42640143
100	—	7.20340190	$-\sqrt{2/101}$	-0.14071951
∞	∞	∞	0	0

Table 2. List of dimensionless collapse times τ , given by Equations (21) and (24), and dimensionless collapse point velocities $\dot{r}(\tau)$, given by Equation (29). Exact solutions are listed if they can be reduced to an algebraic expression with basic constants.

with $\alpha = \eta$, if $\gamma > -1$, and $\alpha = \eta + \frac{1}{2}$, if $\gamma < -1$. We can readily unify these two cases in the single equation

$$\alpha = \frac{1}{4} + \frac{3-\gamma}{4|1+\gamma|}. \quad (19)$$

We have defined α in this way to make the right-hand integral of Equation (18) identical to the definition of the *incomplete beta function*, $B(x; \alpha, \beta) = \int_0^x y^{\alpha-1} (1-y)^{\beta-1} dy$. Hence, Equation (18) solves to

$$t(r) = \tau - \sqrt{\frac{\eta}{2}} B\left(r^{|1+\gamma|}; \alpha, \frac{1}{2}\right). \quad (20)$$

The collapse time τ can be obtained by solving this equation for τ at the point $t = 0$ ($r = 1$),

$$\tau(\gamma) = \sqrt{\frac{\eta}{2}} B\left(\alpha, \frac{1}{2}\right). \quad (21)$$

Here $B(\alpha, \beta)$ with only two arguments is the (complete) *beta function*, i.e., the incomplete $B(x; \alpha, \beta)$ evaluated at $x = 1$. Selected explicit values of τ are listed in Table 2.

Substituting Equation (21) back into Equation (20), the latter can be slightly compacted to

$$t(r) = \sqrt{\frac{\eta}{2}} B\left(1-r^{|1+\gamma|}; \frac{1}{2}, \alpha\right), \quad (22)$$

analogous to the solution for $\gamma > -1$ by [Harrison & Lake \(1972\)](#), but now generalised to all $\gamma \neq -1$.

3.1.2 Special case $\gamma = -1$

What remains is the special case of $\gamma = -1$. Equation (8b) describing this case integrates to

$$t(r) = \tau(-1) \operatorname{erf}\left(\sqrt{-\ln r}\right) \quad (23)$$

where

$$\tau(-1) = \sqrt{\pi/2} \quad (24)$$

is the collapse time, reached for $r \rightarrow 0_+$. This collapse time is equal to the limit of Equation (21) for $\gamma \rightarrow -1$. Likewise, Equation (23) is the limit of Equation (22) for $\gamma \rightarrow -1$.

3.2 Explicit solution $r(t)$

In order to invert the implicit solutions $t(r)$, it is convenient to normalise Equation (20) by τ , which yields

$$\frac{t}{\tau} = 1 - I\left(r^{|1+\gamma|}; \alpha, \frac{1}{2}\right), \quad (25)$$

where $I(x; \alpha, \beta) \equiv B(x; \alpha, \beta)/B(\alpha, \beta)$ is called the *regularised incomplete beta function* (a convenient step pointed out by Roberto Iacono, priv. com.).

The implicit Equations (25) and (23) can be readily inverted to a compact general explicit solution in terms of well-known special functions,

$$r(t) = \begin{cases} Q\left(1 - \frac{|t|}{\tau(\gamma)}; \alpha, \frac{1}{2}\right)^\eta & \text{if } \gamma \neq -1 \\ \exp\left(-\operatorname{erfi}^2\left(\sqrt{2/\pi} t\right)\right) & \text{if } \gamma = -1 \end{cases} \quad (26a)$$

where $\operatorname{erfi}(x)$ is the *inverse error function* and $Q(x; \alpha, \beta)$ is the *inverse regularised incomplete beta function*. As required, Equation (26b) is the limit of Equation (26a) for $\gamma \rightarrow -1$.

The absolute value $|t|$ in Equation (26a) does not follow from Equation (25), only valid for $t \in [0, \tau]$. It is an ad-hoc extension of $r(t)$ to the domain $t \in [-\tau, \tau]$, exploiting the time-reversal symmetry of Equations (5) and (6). Equation (26b) is already time-symmetric. Hence, the solution of Equation (26) is valid on the interval $t \in [-\tau, \tau]$.

The practical value of Equation (26) becomes apparent when realising that the regularised incomplete beta function $I(x; \alpha, \beta)$ is the cumulative density function of the *beta distribution*, a common distribution function in probability theory, related to, but not to be confused with, the beta function. Hence, the function $Q(x; \alpha, \beta)$ is the quantile function of the beta distribution—thus the letter Q . This quantile function is available in all modern computing languages (see Section 3.3 for some examples).

Figure 2 shows $r(t)$ on the interval $t \in [0, \tau(\gamma)]$ for all integer γ from -4 to $+4$. Key properties of these solutions will be discussed in Section 4.

3.3 Code examples

The quantile function $Q(x; \alpha, \beta)$, which forms the heart of the explicit Equation (26a), is readily accessible in programming languages: `qbeta` in R, `scipy.stats.beta.ppf` in PYTHON, `InverseBetaRegularized` in MATHEMATICA, `InvIncompleteBeta` in the ALGLIB library for C++, C#, JAVA, PYTHON, DELPHI; etc. For reference, this section provides a few explicit code examples for plotting the collapse functions shown in Figure 2.

3.3.1 Gravitational spherical top-hat collapse

The gravitational collapse of a uniform pressure-free sphere is governed by Equation (7). The solution $r(t)$ in natural

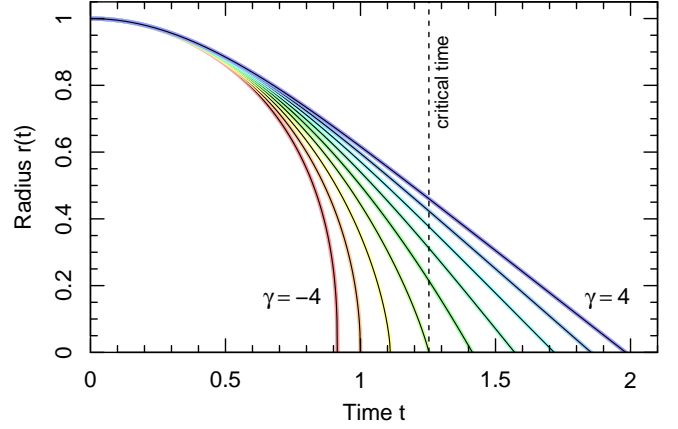


Figure 2. Exact solutions of the normalised collapse Equation (5) with initial conditions of Equation (6), evaluated on the normalised time interval $t \in [0, \tau(\gamma)]$ using the explicit Equation (26). Coloured curves correspond to different values of γ , separated by $\Delta\gamma = 1$. The dashed vertical line marks the collapse time $\sqrt{\pi/2}$, corresponding to the critical exponent $\gamma = -1$ that separates the divergent behaviour of $\dot{r}(\tau)$ from the convergent one.

units R_0 and $T_0 = \sqrt{R_0^3/(GM)}$ is given by Equation (26a) with $\gamma = -2$. Perhaps the most compact implementation is achieved in the statistical language R, where three lines suffice to evaluate and plot this explicit solution:

```
tau = beta(3/2,1/2)/sqrt(2)
r = function(x) qbeta(1-x/tau,3/2,1/2)
curve(r,0,tau,1000)
```

The resulting plot is analogous to the yellow line for $\gamma = -2$ in Figure 2. Most astrophysicists might be more accustomed to PYTHON, where this code could read:

```
import numpy as np
import matplotlib.pyplot as plt
from scipy.stats import beta
from scipy.special import beta as betafct

tau = betafct(3/2, 1/2)/np.sqrt(2)
def r(t):
    return beta.ppf(1-t/tau, 3/2, 1/2)

tvalues = np.linspace(0, tau, 1000)
plt.plot(tvalues, r(tvalues))
plt.show()
```

3.3.2 Ideal spherical cavitation bubble collapse

Readers closer to cavitation dynamics than astrophysics may consider the example of a spherical cavity collapsing in an incompressible liquid of density ρ , without viscosity and surface tension. Assuming a constant driving pressure Δp , the bubble evolution is governed by Equation (10); hence the collapse motion $r(t)$ in natural units R_0 and $T_0 = R_0\sqrt{\rho/\Delta p}$ is given by Equation (26a) with $\gamma = -4$. The corresponding R-script reads:

```
tau = beta(5/6,1/2)/sqrt(6)
r = function(x) qbeta(1-x/tau,5/6,1/2)^(1/3)
curve(r,0,tau,1000)
```


This code reproduces the red line for $\gamma = -4$ in Figure 2. In PYTHON, this could be implemented as:

```
import numpy as np
import matplotlib.pyplot as plt
from scipy.stats import beta
from scipy.special import beta as betafct

tau = betafct(5/6, 1/2)/np.sqrt(6)
def r(t):
    return beta.ppf(1-t/tau, 5/6, 1/2)*(1/3)

tvalues = np.linspace(0, tau, 1000)
plt.plot(tvalues, r(tvalues))
plt.show()
```

3.4 Noteworthy special solutions

For completeness, let us note that for select values of γ , Equation (26) can be reduced to more compact explicit solutions:

$$r(t) = \begin{cases} \sqrt{1-t^2} & \text{if } \gamma = -3 \\ 1-t^2/2 & \text{if } \gamma = 0 \\ \cos(t) & \text{if } \gamma = 1 \\ \text{cn}(t, \frac{1}{2}) & \text{if } \gamma = 3, \end{cases} \quad (27a) \quad (27b) \quad (27c) \quad (27d)$$

where $\text{cn}(x, y)$ is the Jacobi elliptic cosine function.

To my knowledge, Equations (27a–c) are the only explicit closed-form solutions, i.e., solutions in terms of commonly accepted basic functions. These three functions respectively describe an arc of a circle (Equation 27a), a parabola (Equation 27b), and a harmonic oscillation (Equation 27c). Text-book examples for the latter two are given in Table 1.

Equation (27d) is a special case of the undamped and unforced Duffing equation (Duffing 1918), for which general solutions in terms of the Jacobi elliptic family have recently been derived by Salas et al. (2021).

For some other values of γ , parametric solutions, $t(\theta)$ and $r(\theta)$, have been found well before explicit solutions. Arguably, the most famous example is the case of $\gamma = -2$, describing, e.g., the spherical gravitational collapse (see Table 1). In this case (c.f., Lin et al. 1965),

$$t = \frac{\theta + \sin \theta}{\sqrt{8}}, \quad r = \frac{1 + \cos \theta}{2}. \quad (28)$$

Varying θ from 0 to π generates the collapse phase, whereas varying it from $-\pi$ to 0 generates the symmetric growth.

More lengthy parametric solutions have also been presented for other non-trivial cases, such as empty spherical cavitation bubbles ($\gamma = -4$; c.f., Mancas & Rosu 2016).

4 DISCUSSION

The general solution $r(t)$ of Equations (5) and (6) given by Equation (26) warrants a brief discussion. As a preliminary remark, the linear transformation (Equation 3) between the normalised form $r(t)$ and its dimensional analogue $R(T)$ make it straightforward to apply all properties of $r(t)$ to $R(t)$. Moreover, as mentioned in Section 1, any solution of Equations (1) and (2) is invariant under time reversal. This symmetry equally applies to dimensionless coordinates, i.e.,

$r(t) = r(-t)$, for all t , where a solution $r(t)$ exists. For efficiency, I will therefore limit the discussion in this section to the normalised form $r(t)$ and to positive times.

4.1 Behaviour at collapse point

As illustrated in Figure 2, the steepness of the function $r(t)$ monotonically increases as the time sweeps from $t = 0$ ($r = 1$) to the collapse time $t = \tau$ ($r = 0$). Equation (8) shows this immediately and reveals that in the limit $t \rightarrow \tau_-$ ($r \rightarrow 0_+$), the velocity \dot{r} becomes

$$\dot{r}(\tau) = \begin{cases} -\sqrt{\frac{2}{1+\gamma}} & \text{if } \gamma > -1 \\ -\infty & \text{if } \gamma \leq -1 \end{cases}. \quad (29)$$

Some numerical values of $\dot{r}(\tau)$ are listed in Table 2. The divergent behaviour of $\dot{r}(\tau)$ for $\gamma \leq -1$, which can often be interpreted as a positively diverging kinetic energy ($\propto \dot{r}^2$), is mimicked by a negatively diverging potential $\phi(r)$. In fact, following Equation (12),

$$\lim_{r \rightarrow 0_+} \phi(r) = \begin{cases} 0 & \text{if } \gamma > -1 \\ -\infty & \text{if } \gamma \leq -1 \end{cases}, \quad (30)$$

as visualised in Figure 1.

Equations (29) and (30) highlight the existence of two distinct regimes in the domain $\gamma \in \mathbb{R}$, separated by the critical value $\gamma = -1$. This value corresponds to the only singularity of Equation (26a), which can be properly removed by using Equation (26b). The dimensionless collapse time for $\gamma = -1$ is exactly $\sqrt{\pi}/2$ (Equation 24), the value shown by the dashed vertical line in Figure 2. Following Equation (29), all curves reaching $r = 0$ to the left of this line do so vertically, whereas those to the right of the line come down at a finite slope.

The two regimes separated by $\gamma = -1$ often correspond to different classes of physical problems (c.f., Table 1), explaining why—to my knowledge—they have never been addressed simultaneously in previous literature.

The regime $\gamma < -1$, sometimes including $\gamma = -1$, often describes a spherical collapse—gravitational or hydrodynamic in nature (see Table 1). In this case, the collapse motion $r(t)$ near $t = \tau$, is sometimes referred to as ‘violent collapse’ or ‘catastrophic collapse’. This description is quite literal, a saddening example being the implosion of the Titan submersible near the wreck of the Titanic in the North Atlantic Ocean (18 June 2023). This implosion was likely approximated by Equation (1) with $\gamma = -4$, predicting a collapse time $T_c \approx 5\text{ms}$, based on a capsule radius $R_0 \approx 1\text{m}$, a driving pressure $\Delta p \approx 350\text{bar}$ and a water density $\rho \approx 10^3\text{kg m}^{-3}$.

The infinite velocity at the collapse point for $\gamma \leq -1$ is unphysical. Hence, all real-world systems modelled by Equation (1) must start deviating from this model near the collapse point. Secondary mechanisms, which might have been negligible for most of the collapse motion, suddenly become dominant, preventing the singularity. For example, in the case of collapsing cavitation bubbles, these mechanisms include shock waves (liquid compressibility), sonoluminescence, sonochemistry, vapour compression and micro-jetting (see overview by Obreschkow et al. 2013). In the case of matter collapsing by self-gravity, the mechanisms preventing the divergence could be asymmetries, smoothing the collapse point, and pressure forces, possibly enhanced by strong radiation

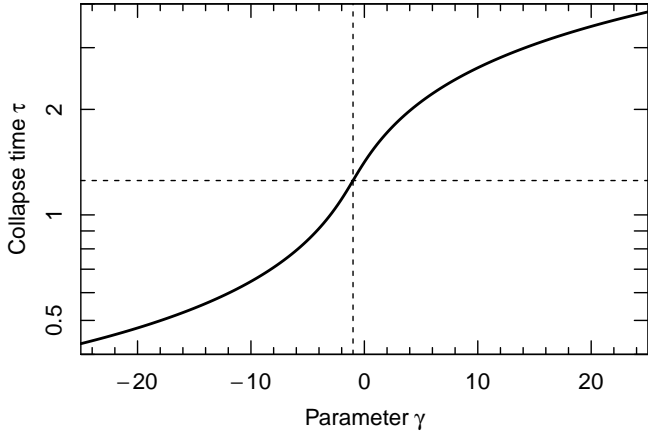


Figure 3. Dimensionless collapse time $\tau = T_c/T_0$ as a function of the control parameter γ . Plotted in semi-log coordinates, this function exhibits a non-trivial point symmetry about $(\gamma = -1, \tau = \sqrt{\pi/2})$, marked by the dashed lines. See Section 4.3.

and phase transitions, e.g., to a neutron star. If these mechanisms cannot prevent $\dot{R}(T)$ from approaching the speed of light, general relativistic effects take over, transforming the collapsing mass into a static black hole (Oppenheimer & Snyder 1939). This is likely the fate of the cores of massive stars ($\gtrsim 25 M_\odot$ Mirabel 2017) and possibly also much more massive ($\sim 10^5 M_\odot$) primordial gas clouds, collapsing directly into black holes (Loeb & Rasio 1994).

4.2 Continuation past collapse point

The solution of Equation (26) is valid only on the interval $t \in [-\tau, \tau]$. However, Equation (5) integrates smoothly past the collapse point $t = \tau$, to negative values of r , if $\gamma \in \mathbb{N}_0$.

For non-negative even γ , the sign of \ddot{r} remains negative as $r < 0$. Hence the ‘collapse’ motion continues through the point $t = \tau$ with ever increasing velocity, such that $\lim_{t \rightarrow \infty} \dot{r} = -\infty$. The simplest example would be an object dropped to the ground (defined as $R = 0$) into a vertical shaft ($R < 0$) with constant acceleration g ($\gamma = 0$, see Table 1).

For positive odd γ , however, $r(t)$ passes through $r(\tau) = 0$, while inverting the sign of \ddot{r} . Symmetry considerations imply that $r(t)$ then describes an oscillating curve of wavelength $\lambda = 4\tau$, made of reflections of the arc $r(t \in [0, \tau])$. This curve satisfies $r(0) = 1$, $r(\tau) = 0$, $r(2\tau) = -1$, $r(3\tau) = 0$, $r(4\tau) = 1$, and so forth. For $\gamma = 1$, the oscillation is harmonic (Equation 27c), for all larger odd γ , it is anharmonic.

Non-real positive $\gamma \in \mathbb{R}_+$ would generally lead to complex solutions $r(t) \in \mathbb{C}$, if integrated past the collapse point. In fact, immediately past the collapse point, the acceleration has the complex argument $\arg(\ddot{r}) = (\gamma+1)\pi$; hence the imaginary component of \ddot{r} only vanishes for integer γ .

For negative γ (integer or real), Equation (26) diverges as $r \rightarrow 0$. This is a coordinate singularity, which can, in principle, be removed through regularisation techniques.

4.3 γ - τ Symmetry

Figure 3 shows the dimensionless collapse time τ as a function of the control parameter γ . With τ on a logarithmic axis, this function becomes an S-shape, which owes its symmetry

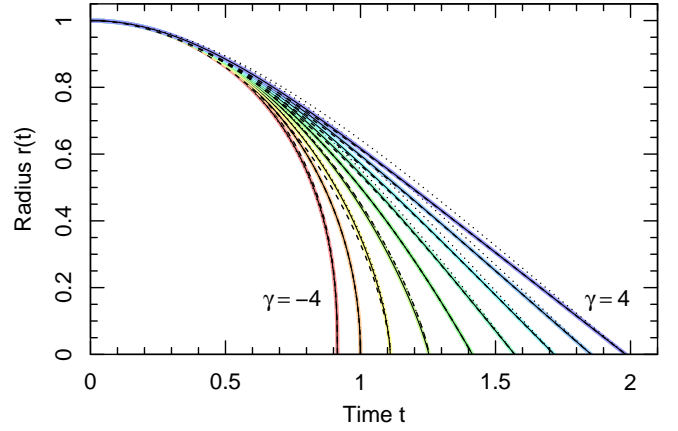


Figure 4. Exact versus approximate solutions of the normalised collapse equation Equation (5) with initial conditions of Equation (6), evaluated on the normalised time interval $t \in [0, \tau(\gamma)]$. The selected values of γ are the same as in Figure 2. Solid lines are the exact solutions given in Equation (26), whereas dashed and dotted lines use the approximation of Equation (32) with parameters p_1 and q_1 (dashed) and p_2 and q_2 (dotted).

to a well-known identity for Beta functions, $B(\alpha, \beta)B(\alpha + \beta, 1 - \beta) = \pi/(\alpha \sin(\pi\beta))$. Applied to Equation (21), this identity implies that any point $(\gamma, \tau(\gamma))$ can be mapped onto a corresponding point

$$(\gamma, \tau) \mapsto \left(\gamma' = -2 - \gamma, \tau' = \frac{\pi}{2\tau} \right), \quad (31)$$

which also lies on the function $\tau(\gamma)$. The only invariant point of this symmetry transformation, $(\gamma = -1, \tau = \sqrt{\pi/2})$, is marked by the dashed lines in Figure 3. This point coincides with the special case of Equation (24). It is the point, at which Equation (26a) becomes singular and where $\dot{r}(0)$ transitions from a finite to a diverging value (Section 4.1).

The symmetry Equation (31) does not have a straightforward known extension to general times $t \neq \tau$, say in the shape of $(\gamma, t, r) \mapsto (\gamma', t', r')$. Hence, the two branches of solutions for $\gamma < -1$ (with diverging \dot{r}) and $\gamma > -1$ (with finite \dot{r}) cannot easily be expressed in terms of each other.

4.4 Polynomial approximations

In some practical cases, it may be useful and sufficient to substitute the exact solution $r(t)$ given in Equation (26) by simple approximations $\tilde{r}(t)$. A possible choice is

$$\tilde{r}(t) = \begin{cases} (1 - x^2)^p & \text{if } \gamma \leq -1 \\ q(1 - |x|) - (q-1)(1 - |x|)^{\frac{q}{q-1}} & \text{if } \gamma > -1, \end{cases} \quad (32a)$$

$$(32b)$$

where $x = t/\tau$ (with τ given in Equations (21) and (24)) and where $p \in (0, 1)$ and $q > 1$ are shape parameters.

These are arguably the simplest polynomials, which simultaneously satisfy six essential properties of the exact solution: (1) time symmetry, $\tilde{r}(t) = \tilde{r}(-t)$ if $t \in [-\tau, \tau]$; (2) negative curvature $\ddot{\tilde{r}}(t) < 0$ if $t \in (-\tau, \tau)$, (3) $\tilde{r}(0) = 1$; (4) $\tilde{r}(\tau) = 0$; (5) $\dot{\tilde{r}}(0) = 0$; and (6) $\lim_{t \rightarrow \tau} \dot{\tilde{r}}(t)$ is finite if and only if $\gamma > -1$.

Choosing the exponent p equal to $p_1 = 2/(1 - \gamma)$ (for γ strictly below -1) ensures the correct asymptotic behaviour of $\dot{\tilde{r}}$ as a function of \tilde{r} in the limit $t \rightarrow \tau$. This approximation was presented by Obreschkow et al. (2012) for $\gamma = -4$ (thus

$p = 2/5$). Equation (32a) can then be seen as the first term in a rapidly converging series, which tends towards the true solution if using the exact coefficients of Amore & Fernández (2013). Alternatively, setting p equal to $p_2 = \tau^2/2$, satisfies $\ddot{r}(0) = \dot{r}(0) = -1$. Likewise, the parameter q can be set to $q_1 = \eta B(\eta, \frac{1}{2})$ (with η defined in Equation 16) to ensure that $\dot{r}(\tau) = \dot{r}(\tau)$, or equal to $q_2 = \tau^2/(\tau^2 - 1)$ to ensure $\ddot{r}(0) = \ddot{r}(0) = -1$.

As shown in Figure 4, both of the above choices for p and q provide reasonable approximations of the exact solution. In general, the best pick depends on the application. If $\gamma = -3$ (hence $p_1 = p_2 = \frac{1}{2}$) or $\gamma = 0$ (hence $q_1 = q_2 = 2$), the two options are identical and Equation (32) is equal to the exact solutions of Equations (27a) and (27b), respectively.

A more quantitative discussion of the approximations is beyond the scope of this paper, but can be found in Obreschkow et al. (2012) and Amore & Fernández (2013) for $\gamma = -4$.

5 CONCLUSION

This paper investigated the differential Equation (1) with boundary conditions stated in Equation (2). One might call this the spherical collapse equation in reference to its most common applications (c.f., Table 1).

I have shown that this collapse equation exhibits a unified explicit solution, conveniently expressed in dimensionless coordinates $\{r = R/R_0, t = T/T_0\}$. Elements of its derivation can be found elsewhere, spread over decades of literature across several unrelated fields. The contribution of this work is to unify previously known parametric, implicit and explicit solutions from hydrodynamics (c.f., Rayleigh-Plesset equation), hydrostatics (Lane-Emden equation) and astrophysics (top-hat spherical collapse model), all limited to different subsets of γ , into a single concise solution (Equation 26a), universally valid for all real $\gamma \neq -1$. For $\gamma = -1$ this solution is singular, but its limit $\gamma \rightarrow -1$ exists and is given in Equation (26b).

The existence of a general explicit solution is barely known, particularly in astrophysics and cosmology, where only parametric solutions like Equation (28) are commonly taught. I suspect this is because in the day when analytic argument was more mainstream, beta distributions would have been no easier to deal with than parametric solutions; and in the modern day, where beta distributions are readily accessible, the need for using them is less pressing, since numerical integration has become cheap.

The explicit solution $r(t)$ is not just more elegant and faster to evaluate than numerical integration, but it also offers: (i) a mathematical unification of seemingly unrelated physical applications (c.f., Table 1); (ii) interesting insights, for example pertaining to symmetry properties (Section 4.3); and (iii) a view on a hidden connection between the spherical collapse equation and probability theory, via the appearance of the beta distribution in Equation (26a). The explicit solution can provide exact benchmarks for testing numerical integration techniques and simulation codes, e.g., for hydrodynamic and gravitational simulations.

An interesting avenue for research in pure mathematics is an extension to complex-valued functions $r(t)$, where additional symmetries in the complex plane exist for $\gamma \in \mathbb{N}$.

ACKNOWLEDGEMENTS

I thank Dr. Martin Bruderer and Dr. Aaron Ludlow for insightful suggestions that have improved this work. I am also grateful to Dr. Roberto Iacono for bringing to my attention the convenience of using the regularised incomplete beta function in transitioning from Equation (22) to Equation (26a), bypassing a somewhat more cumbersome earlier method temporarily invoking the hypergeometric function. Last but not least, I extend my gratitude to Dr. Mohamed Farhat and Prof. Andrea Prosperetti for many past discussions, which were a source of inspiration in writing this paper. I am a recipient of an Australian Research Council Future Fellowship (FT190100083) funded by the Australian Government.

DATA AVAILABILITY

No new data were generated or analysed in support of this research.

REFERENCES

- Amore P., Fernández F. M., 2013, The Journal of Chemical Physics, 138, 084511
- Duffing G., 1918, Erzwungene Schwingungen bei veränderlicher Eigenfrequenz und ihre technische Bedeutung, Series: Sammlung Vieweg No. 41-42. Vieweg & Sohn
- Emden R., 1907, Gaskugeln. Leipzig: B. G. Teubner
- Gunn J. E., Gott J. Richard I., 1972, ApJ, 176, 1
- Harrison E. R., Lake R. G., 1972, ApJ, 171, 323
- Klotz A. R., 2013, Physics of Fluids, 25, 082109
- Kudryashov N. A., Sinelshchikov D. I., 2014, Journal of Physics A: Mathematical and Theoretical, 47, 405202
- , 2015, Physics Letters A, 379, 798
- Lane H. J., 1870, American Journal of Science, 50, 57
- Lin C. C., Mestel L., Shu F. H., 1965, ApJ, 142, 1431
- Loeb A., Rasio F. A., 1994, ApJ, 432, 52
- Mancas S. C., Rosu H. C., 2016, Physics of Fluids, 28
- Mirabel F., 2017, New Astron. Rev., 78, 1
- Obreschkow D., Bruderer M., Farhat M., 2012, Phys. Rev. E, 85, 066303
- Obreschkow D., Tinguely M., Nicolas D., Philippe K., de Bosset Aurele, Mohamed F., 2013, Experiments in Fluids, 54
- Oppenheimer J. R., Snyder H., 1939, Physical Review, 56, 455
- Rayleigh L., 1917, Phil. Mag., 34, 94
- Salas A. H., Castillo Hernández J. E., Martínez Hernández L. J., 2021, Mathematical Problems in Engineering, 2021
- Slepian Z., Philcox O. H. E., 2023, Monthly Notices of the Royal Astronomical Society: Letters, 522, L42
- Stokes G., 1847. Notebook preserved in the Cambridge University Library, Add. MS. 7656. NB23.